Instantaneous Feedback Control for a Fuel-Prioritized Vehicle Cruising System on Highways With a Varying Slope

Shaobing Xu, Shengbo Eben Li, *Member, IEEE*, Bo Cheng, and Keqiang Li

***Abstract*—This paper presents two fuel-prioritized feedback controllers, which are called the estimated minimum principle (EMP) and kinetic energy conversion (KEC), to realize eco-cruising on varying slopes for vehicles with conventional powertrains. The former is derived from the minimum principle with an estimated Hamiltonian, and the latter is designed based on the equivalent conversion between the kinetic-energy change of vehicle body and the fuel consumption of the engine. They are implemented with analytical control laws and rely on current road slope information only without look-ahead prediction. This feature results in a very light computing load, with the average computing time of each step less than one millisecond. Their fuel-saving performances are quantitatively studied and compared with a model predictive control and a constant speed control. As an expansion, the control rule for avoiding rear-end collision is also designed by using a safety-guaranteed car-following model to constrain the high-risk behaviors.**

***Index Terms*—Automated vehicle, eco-driving, fuel economy, optimal control.**

I. Introduction

TIGHTENING fuel economy standards and concerns on environment continue to pressure the automotive industry to improve the fuel economy of road vehicles [1]. Technologies such as clean combustion, lightweight, hybrid powertrain, and intelligent transportation system have been continuously developed and deployed [2], [3]. Besides enhancing powertrain efficiency, how to operate a vehicle also significantly affects the fuel economy, which forms the so-called eco-driving technique. It aims to improve fuel economy by optimizing driving/control strategies without changing vehicular structure.

The key of eco-driving technique is the fuel-saving control strategies. In this paper, we focus on fuel-prioritized cruising (or eco-cruising) control on highways considering varying road slope. Cruising, as a common driving maneuver, consumes a considerable portion of total energy, e.g., 35% under urban conditions [4], and higher on highways. It is estimated that a 1% fuel savings in cruising scenario can save 20 million barrels of oil per year world-wide [2]. Road slope is an unnegligible factor to design eco-cruising controller, by which the vehicle should actively adjust its speed to improve engine efficiency and decrease aerodynamic drag for saving fuel [5], [6].

Three categories of methods are usually involved for the eco-cruising control on varying slope: global optimization, look-ahead control, and instantaneous control. The global optimization is to obtain the optimal solution of whole horizon by methods such as dynamic programming. Due to its heavy computing load and deficiency on handling uncertainty such as the frontal vehicles, this method is less practical for the real traffic system and usually used as a benchmark [7]. As an evolution, the look-ahead control, also called as model predictive control (MPC), is widely used for the eco-cruising system in the existing works. It adopts the upcoming slope information in a finite receding horizon to optimize the vehicle speed profile by repeatedly solving an optimal control problem [8]. For example, Nielsen *et al.* presented a look-ahead controller to minimize both fuel consumption and trip time for heavy trucks considering road slope [5]. The dynamic programming was used to numerically solve the optimal control problem at each step and about 3.5% fuel reduction was observed. Di Cairano and Borhan *et al.* designed different MPC controllers for the energy management of hybrid electric vehicles (HEVs), and further discussed their fast solving algorithms and theories for stochastic systems [9], [10]. Other related works can be found in [6], [11]–[14]. Even though achieved desirable fuel benefit, the MPC suffers high computing load in engineering practice, especially for nonlinear constrained problems. Boyd *et al.* pointed out that MPC could be used for slow systems only whose sample time is measured in seconds or minutes [15].

To be more practical, the instantaneous control that relies on current vehicle state and road information to generate control inputs instead of online solving optimal control problems, is a common approach that has been used in real applications [16]. It has lower computing load and better reliability as compared with the information-rich computationally heavy controllers such as the MPC. The instantaneous control is widely used in power management of HEVs, such as the rule-based method and the equivalent consumption minimization strategy (ECMS) [7], [17], e.g., Rizzoni *et al.* proposed an adaptive ECMS strategy with pointing out that its performance is pretty close to the global optimal result of dynamic programming [16].

This paper aims to develop the instantaneous-type eco-cruising controller for conventional vehicles equipped with

Manuscript received September 14, 2015; revised January 23, 2016 and June 8, 2016; accepted August 10, 2016. Date of publication September 13, 2016; date of current version May 1, 2017. This work was supported by the National Science Foundation of China under Grant 51575293. The Associate Editor for this paper was F.-Y. Wang. *(Shaobing Xu and Shengbo Eben Li contributed equally to this work.)*

The authors are with the State Key Laboratory of Automotive Safety and Energy, Department of Automotive Engineering, Tsinghua University, Beijing 100084, China (e-mail: xsbing2008@foxmail.com; lisb04@gmail.com; chengbo@tsinghua.edu.cn; likq@mail.tsinghua.edu.cn).

Color versions of one or more of the figures in this paper are available online at http://ieeexplore.ieee.org.

Digital Object Identifier 10.1109/TITS.2016.2600641

an internal combustion engine and an automated mechanical transmission (AMT). Different from the cooperative control of motor and engine for HEVs, the eco-cruising control for conventional vehicles on varying slope is to optimize the vehicle speed profile by manipulating the engine, transmission, and brake system. To avoid time-costly online numerical optimization, we focus on the instantaneous feedback control that uses current road slope only instead of predictive road information, which could be able to yield analytical control laws for real time implementation. An earlier study for carburetor-based vehicles can be found in [18]. To achieve the purposes of fast eco-cruising control, the central issue is how to design analytical control laws for the mixed-integer system with an highly nonlinear engine and discrete gear ratio, which leads to a challenging mixed-integer problem [19], [20].

The contribution of this paper is to design two real-time feedback controllers, i.e., estimated minimum principle (EMP) and kinetic energy conversion (KEC), to realize eco-cruising control on varying slope for the conventional vehicles. The fuel-saving control issue is formulated as a Lagrange-type optimal control problem in the spatial domain. The EMP is derived from the Pontryagin's minimum principle with an estimated Hamiltonian, and the KEC is designed based on equivalent conversion between the kinetic energy of vehicle body and the fuel consumption of engine. Both of them yield analytical control laws with computing time of each step in the level of one millisecond, making them suitable for online implementation. Their fuel-saving performances are quantitatively compared with an optimization-based MPC and a constant speed (CS) control. Considering the scenario of impeded by a slow frontal vehicle, the EMP and KEC are expanded by using a safety-bounded car-following model to constrain the high-risk behaviors, which enables rear-end collision avoidance.

The rest of this paper is organized as follows: Section II formulates the eco-cruising control problem; Section III designs the two feedback controllers, i.e., EMP and KEC; Section IV compares and analyzes their performances; Section V extends the two controllers to car-following scenario, and Section VI concludes this paper.

II. Problem Statement

With precise digital map and GPS, the information of road slope could be collected and applied to improve the fuel economy for automated vehicles, as shown in Fig. 1. The goal of an eco-cruising system is to minimize the total fuel consumption under safety constraints while running in a given speed range. The controller to determine proper engine power, transmission gear, and brake force is the key part of the eco-cruising system. This paper focuses on designing eco-cruising controllers for vehicles with AMT whose gear ratio is discrete. The eco-cruising problem naturally casts into the optimal control framework. The vehicle dynamics and engine fuel model are described as follows.

A. Vehicle Longitudinal Dynamics for Control

The studied vehicle is equipped with an internal combustion engine, AMT, and wet clutch. The following assumptions

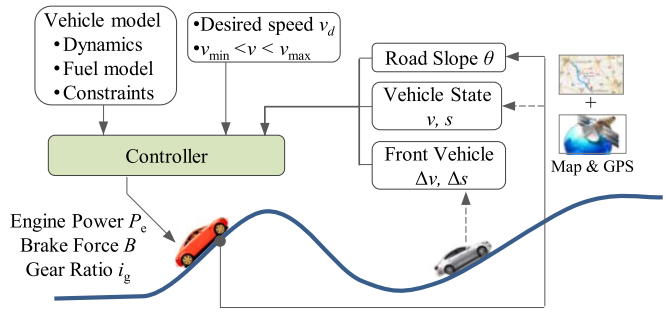

Fig. 1. Eco-cruising control system on varying slope.

are made to tradeoff between conciseness and accuracy: (a) the dynamics of flywheel and transmission are ignored; (b) the efficiency of AMT is a constant on all gears, and the gear shifting is executed instantaneously; (c) the rolling resistance coefficient is a constant, even though it is related to the vehicle speed [21]. The applied vehicle longitudinal model is then described as

$$\begin{aligned}
\dot{s} &= v, \\
\dot{v} &= a = g(\cdot), \\
g(\cdot) &= \frac{1}{M}\left(\frac{\eta_{\mathrm{T}} P_{\mathrm{e}}}{v} + B - r(v) - h(s)\right), \\
P_{\mathrm{e}} &= T_{\mathrm{e}} w_{\mathrm{e}} \\
r(v) &= k_a v^2, \\
h(s) &= Mg\left(f\cos\theta(s) + \sin\theta(s)\right),
\end{aligned} \tag{1}$$

where s, v, and a are the distance, speed, and acceleration; M is the vehicle mass; η_{T} is the efficiency of AMT; P_{e}, T_{e}, and w_{e} are the engine power, torque, and speed, respectively; B is the brake force; $r(v)$ represents the aerodynamic drag, and k_a is the lumped coefficient; $h(s)$ stands for the rolling resistance and gradient resistance, f is the rolling resistance coefficient and θ is the road slope.

To facilitate the controller designing, the above temporal dynamics are converted into spatial domain when $v > 0$, i.e.,

$$\frac{\mathrm{d}v}{\mathrm{d}s} = \frac{1}{v} g(P_{\mathrm{e}}, B, v, s). \tag{2}$$

The vehicle speed v and the engine speed w_{e} are governed by

$$w_{\mathrm{e}} = k_w v i_{\mathrm{g}}, \tag{3}$$

where k_w is the lumped coefficient; i_{g} is the gear ratio of AMT, which is a discrete variable, i.e.,

$$i_{\mathrm{g}} \in \{i_{\mathrm{g1}}, i_{\mathrm{g2}}, i_{\mathrm{g3}}, i_{\mathrm{g4}}, i_{\mathrm{g5}}\}. \tag{4}$$

The engine speed w_{e}, engine torque T_{e}, and brake force B are constrained by their physical limits, as shown in (8), where B_{lim} (negative) is the boundary of brake force. In reality, drivers usually have a desired speed range to limit the speed level when cruising on a varying slope, i.e.,

$$v_{\min} \le v \le v_{\max}. \tag{5}$$

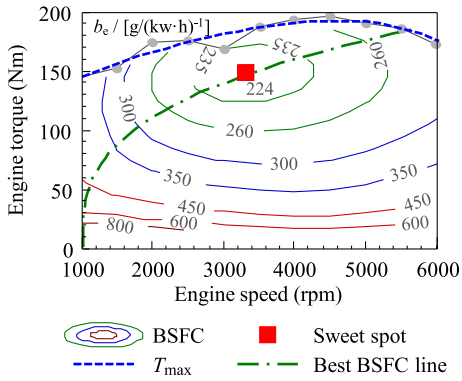

Fig. 2. Engine model.

B. Engine Fuel Model for Control

The total fuel consumption J of cruising to a specific destination is defined as

$$J = \int_{s_0}^{s_f} \frac{\mathcal{F}_e(\cdot)}{v} \mathrm{d}s, \tag{6}$$

where s_0/s_f is the initial/final distance; $\mathcal{F}_e(\cdot)$ is the engine fuel injection rate, which is described by a 2-dimensional 4th-order polynomial [20], i.e.,

$$\mathcal{F}_e(T_e, w_e) = \sum_{i=0}^{4} \sum_{j=0}^{i} k_{i,j} T_e^{i-j} w_e^j, \tag{7}$$

where $k_{i,j}$ are the fitting coefficients. The engine brake specific fuel consumption (BSFC) is shown in Fig. 2, along with the sweet spot, best BSFC line, and maximum torque $T_{\max}$.

C. Optimal Control Problem of Eco-Cruising

The optimal control problem of eco-cruising on varying slope for the AMT-type vehicle is formulated as

$$\min\ J = \int_{s_0}^{s_f} \frac{\mathcal{F}_e}{v} \mathrm{d}s,$$

subject to

$$\begin{aligned}
\frac{\mathrm{d}v}{\mathrm{d}s} &= \frac{1}{v} g(P_e, B, v, s), \\
i_g &\in \{i_{g1}, i_{g2}, i_{g3}, i_{g4}, i_{g5}\}, \\
P_e &= w_e T_e, \\
w_e &= k_w v i_g \\
w_{\min} &\le w_e \le w_{\max}, \\
0 &\le T_e \le T_{\max}(w_e), \\
B_{\lim} &\le B < 0, \\
v_{\min} &\le v \le v_{\max}.
\end{aligned} \tag{8}$$

In this problem (8), the control inputs are the engine power P_e, gear ratio i_g, and brake force B; the state is the vehicle speed v. The involved parameters of engine model and vehicle dynamics are listed in Table I.

TABLE I
KEY PARAMETERS OF VEHICLE DYNAMICS

Parameters	Value	Parameters	Value
M	1600 kg	$w_{\min}$	1000 rpm
η_T	0.90	$w_{\max}$	6000 rpm
k_a	0.43	$B_{\lim}$	-6000 N
f	0.028	k_b	11.133 Nm/(rpm$^{1/3}$)
k_w	120.16	k_e	1/3
a_0, a_1, a_2	3.048 g/s, 0.0905 g/(s·kW), 0.00148 g/(s·kW^2)		
i_g	3.620, 1.925, 1.285, 0.933, 0.692		

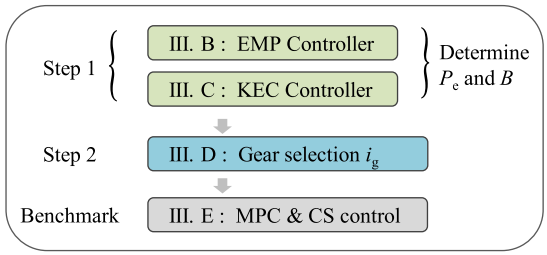

Fig. 3. Structure of the controller designing.

III. Controller Design

This section focuses on designing two feedback controllers, called as Estimated Minimum Principle (EMP) and Kinetic-Energy Conversion (KEC).

A. Framework of Controller Designing

The goal of problem (8) is to obtain proper engine power P_e, brake force B, and gear ratio i_g to improve the fuel economy of cruising on varying slope. Due to the discrete gear ratio i_g, the problem (8) is a highly nonlinear mixed-integer problem, which is challenging to solve. This feature makes the controller designing more difficult. Therefore, in this paper we first determine the optimal engine power P_e^* and brake force B^* with assuming that the gear ratio is continuous as an ideal CVT, and then select the gear ratio i_g of AMT under the determined engine power P_e^*. This strategy converts the optimization of P_e, B, and i_g into two sub-steps, i.e.,

- **Step 1**: Optimize the engine power P_e and brake force B with assuming the discrete gear ratio as a continuous one, which makes the problem (8) become a continuous control problem.
- **Step 2**: Based on the optimized P_e^*, determine a best transmission gear that could maximize the fuel economy.

Even though this strategy makes the results of P_e, B, and i_g lose global optimality, it is practical and could achieve roughly similar fuel-saving performance as compared with MPC, which is verified by the following simulation results. The rest of Section III is organized as Fig. 3: two controllers for step 1 are presented in Section III-B and C, the gear selection for step 2 is introduced in Section III-D, followed by two benchmarks in Section III-E.

Under the assumption of continuous gear ratio, the engine can operate on the best BSFC line [22], a collection of the most

efficient points for varying power level, as shown in Fig. 2, to maximize the engine fuel efficiency. It is described by

$$T_{\mathrm{e}}(w_{\mathrm{e}}) = k_b(w_{\mathrm{e}} - 1000)^{k_{\mathrm{e}}}, \tag{9}$$

where k_b and k_{e} are the fitting coefficients. Then the engine fuel injection rate depends on the engine power only, and can be simplified as the widely used VT-CPFM1 model [23], i.e.,

$$\mathcal{F}_{\mathrm{e}}(P_{\mathrm{e}}) = a_0 + a_1 P_{\mathrm{e}} + a_2 P_{\mathrm{e}}^2, \quad P_{\mathrm{e}} \geq 0 \tag{10}$$

where $a_{\#}$ are the fitting coefficients. Note that this model is less accurate at some operating points, thus it is used for controller designing only, and the real engine fuel is estimated by the BSFC map in the following case studies.

B. Estimated Minimum Principle (EMP) Controller

The Pontryagin's minimum principle is applied to analyze the continuous eco-cruising problem for obtaining a feedback control law. Its Hamiltonian is defined as

$$H = \frac{\mathcal{F}_{\mathrm{e}}(P_{\mathrm{e}})}{v} + \lambda \frac{g(P_{\mathrm{e}}, B, v, s)}{v}. \tag{11}$$

The optimal control is the one that minimizes the Hamiltonian. If P_{e} is free without bounds, we can obtain the necessary conditions of optimality, i.e.,

$$\begin{aligned} \frac{\partial H}{\partial P_{\mathrm{e}}} &= \frac{1}{v}\left(\frac{\partial \mathcal{F}_{\mathrm{e}}(P_{\mathrm{e}})}{\partial P_{\mathrm{e}}} + \lambda \frac{\eta_{\mathrm{T}}}{Mv}\right) = 0, \\ \frac{\partial H}{\partial B} &= \frac{\lambda}{Mv} = 0, \end{aligned} \tag{12}$$

where

$$\frac{\partial \mathcal{F}_{\mathrm{e}}(P_{\mathrm{e}})}{\partial P_{\mathrm{e}}} > 0. \tag{13}$$

However, since the engine power is limited by $P_{\mathrm{e}} \in [0, P_{\mathrm{e,max}}]$, Eq. (12) is not always satisfied. By using the minimum principle, we have

(a) if $(\partial H/\partial P_{\mathrm{e}}) < 0 \Longrightarrow -(Mv/\eta_{\mathrm{T}})(\partial \mathcal{F}_{\mathrm{e}}/\partial P_{\mathrm{e}}) > \lambda \Longrightarrow P_{\mathrm{e}} = P_{\mathrm{e,max}}, B = 0$

(b) if $(\partial H/\partial P_{\mathrm{e}}) = 0 \Longrightarrow -(Mv/\eta_{\mathrm{T}})(\partial \mathcal{F}_{\mathrm{e}}/\partial P_{\mathrm{e}}) = \lambda \Longrightarrow P_{\mathrm{e}} \in [0, P_{\mathrm{e,max}}], B = 0$

(c) if $(\partial H/\partial P_{\mathrm{e}}) > 0 \Longrightarrow$

(c.1) $-(Mv/\eta_{\mathrm{T}})(\partial \mathcal{F}_{\mathrm{e}}/\partial P_{\mathrm{e}}) < \lambda < 0 \Longrightarrow P_{\mathrm{e}} = 0, B = 0$

(c.2) $0 = \lambda \Longrightarrow P_{\mathrm{e}} = 0, B \in [B_{\mathrm{lim}}, 0]$

(c.3) $0 < \lambda \Longrightarrow P_{\mathrm{e}} = 0, B = B_{\mathrm{lim}}$

In the following, we first consider the scenario (b). The minimum Hamiltonian is noted as μ, then

$$\frac{\mathcal{F}_{\mathrm{e}}(P_{\mathrm{e}}^*)}{v} - \frac{M}{\eta_{\mathrm{T}}} \frac{\partial \mathcal{F}_{\mathrm{e}}}{\partial P_{\mathrm{e}}^*} g(P_{\mathrm{e}}^*, 0, v, s) = \mu. \tag{14}$$

It can be simplified as

$$\mathcal{F}_{\mathrm{e}}(P_{\mathrm{e}}^*) - \frac{\partial \mathcal{F}_{\mathrm{e}}}{\partial P_{\mathrm{e}}^*} P_{\mathrm{e}}^* = \mu v - \frac{\partial \mathcal{F}_{\mathrm{e}}}{\partial P_{\mathrm{e}}^*} P_{\mathrm{d}}(v), \tag{15}$$

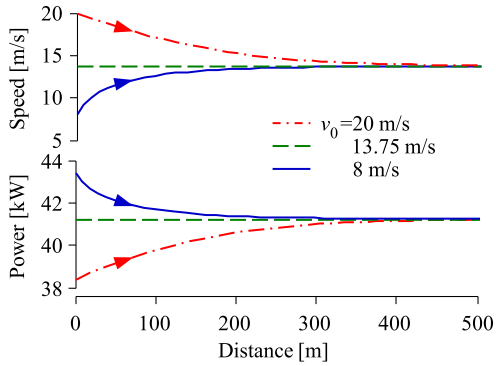

Fig. 4. Vehicle speed and engine power profiles of the EMP controller with different initial speeds on a fixed slope.

where $P_{\mathrm{d}}(v)$ is the demanded power of cruising at fixed speed v on slope θ, i.e.,

$$P_{\mathrm{d}}(v) = \frac{v}{\eta_{\mathrm{T}}}\left[r(v) + h(s)\right]. \tag{16}$$

Taking the engine fuel model (10) into (15), we get the analytical solution of P_{e}^*, i.e.,

$$P_{\mathrm{e}}^* = P_{\mathrm{d}} \pm \sqrt{\frac{-v\mu + \mathcal{F}_{\mathrm{e}}(P_{\mathrm{d}})}{a_2}}. \tag{17}$$

However, in this highly nonlinear constrained problem, the optimal Hamiltonian μ is still challenging to be obtained. Here we adopt an alternative $\overline{\mu}$ to approximate the optimal μ, with $\overline{\mu}$ defined as

$$\overline{\mu} = \frac{\mathcal{F}_{\mathrm{e}}(\overline{P}_{\mathrm{d}})}{\overline{v}(\theta)}, \tag{18}$$

where $\overline{v}(\theta)$ is the MPG (miles per gallon)-maximized speed of cruising on a fixed slope θ using a constant speed, and $\overline{P}_{\mathrm{d}}$ is the corresponding demanded power. The term $\overline{\mu}$ is actually the Hamiltonian of steady-state cruising on the constant slope, meaning the lowest "fuel per meter" of cruising on fixed slope θ. We use this estimated Hamiltonian to approximate the unknown optimal Hamiltonian μ, even though it leads to a non-optimal solution. Applying this approximation, the optimal control P_{e}^* in (17) can be converted to

$$P_{\mathrm{e}}^* = P_{\mathrm{d}} \pm \sqrt{\frac{-v\,\mathcal{F}_{\mathrm{e}}(\overline{P}_{\mathrm{d}}) + \overline{v}\,\mathcal{F}_{\mathrm{e}}(P_{\mathrm{d}})}{\overline{v} a_2}}. \tag{19}$$

In (19), if $v \geq \overline{v}$, select "$-$", otherwise select "$+$". If $v = \overline{v}$, $P_{\mathrm{e}}^* = P_{\mathrm{d}}$. To better understand this controller, an example is given below: the vehicle cruises on a long fixed slope, e.g., $\theta \equiv 8^\circ$, whose corresponding $\overline{v}(\theta)$ is 13.75 m/s. With the initial speed set to 8, 13.75, or 20 m/s, the vehicle speed and engine power profiles are obtained by this controller as shown in Fig. 4. This result indicates that the controller can make the vehicle speed converge to $\overline{v}(\theta)$ in an economical way if the initial speed deviated.

If the calculated $P_{\mathrm{e}}^* > P_{\mathrm{e,max}}$, then P_{e}^* is set to $P_{\mathrm{e,max}}$. This case corresponds to the scenario (a). If $P_{\mathrm{e}}^* < 0$ and $v < v_{\max}$, then $P_{\mathrm{e}}^* = 0$ (idling) and $B = 0$, corresponding to the scenario (c.1). If the vehicle speed tends to exceed the maximum speed

$v_{\max}$ without engine output, the brake operation is executed; this case corresponds to the scenario (c.2) and (c.3).

C. Kinetic-Energy Conversion (KEC) Controller

At any instant, the vehicle can either be driven by consuming fuel or coast by depleting the kinetic energy of vehicle body. Actually, both the engine fuel and the vehicle kinetic energy can be regarded as energy source. The KEC controller is to determine which one is more efficient and then decide to use fuel, or kinetic energy, or both of them synchronously.

To understand this idea, an optimization problem at an instant is formulated: during time Δt, the vehicle speed changes from v to $v+\Delta v$ with a fixed acceleration a; the engine power is P_{e} and the fuel consumption is $\mathcal{F}_{\mathrm{e}}(P_{\mathrm{e}})\Delta t$. To minimize the fuel consumption in Δt, a radical strategy is to turn off the engine, and the kinetic energy is used with the vehicle speed decreasing. However, this strategy cannot maximize the fuel economy since the speed reduction is ignored. In the following optimization, a correction term is added to the performance index to take the change of kinetic energy ΔE into account, i.e.,

$$\min_{P_{\mathrm{e}}} J=\frac{\mathcal{F}_{\mathrm{e}}(P_{\mathrm{e}})\Delta t-\gamma\Delta E}{v\Delta t}, \tag{20}$$

where $\Delta E=Mva\Delta t$; γ is the coefficient of converting kinetic energy to fuel, which could be regarded as the "price" of kinetic energy. It depends on two factors: (1) the engine efficiency by which the kinetic energy is generated; (2) the effective or usable proportion of the kinetic energy, because a higher kinetic energy or vehicle speed always means a higher aerodynamic drag. Namely, the "price" of high kinetic energy is cheaper since a higher proportion of them are wasted. In this paper, γ is designed as

$$\gamma=\frac{1}{\eta_{\mathrm{T}}\eta_{\mathrm{est}}}\frac{h(s)}{h(s)+r(v)}\frac{1}{c_{\mathrm{g}}}, \tag{21}$$

where η_{est} is the estimated engine efficiency and set to 35% here, c_{g} is the calorific value of gasoline.

In the problem (20), the optimal engine power meets that

$$\frac{\mathrm{d}J}{\mathrm{d}P_{\mathrm{e}}}=0. \tag{22}$$

Thus

$$\frac{\mathrm{d}\mathcal{F}_{\mathrm{e}}(P_{\mathrm{e}})}{\mathrm{d}P_{\mathrm{e}}}-\frac{1}{\eta_{\mathrm{est}}c_{\mathrm{g}}}\frac{h}{h+r}=0. \tag{23}$$

Taking the engine fuel model (10) into (23), we have

$$P_{\mathrm{e}}^{*}=\frac{1}{2a_2}\left(\frac{1}{\eta_{\mathrm{est}}c_{\mathrm{g}}}\frac{h}{h+r}-a_1\right). \tag{24}$$

If the calculated $P_{\mathrm{e}}^{*}>P_{\mathrm{e,max}}$, set $P_{\mathrm{e}}^{*}=P_{\mathrm{e,max}}$. If the vehicle cruises on a downhill with $P_{\mathrm{e}}^{*}<0$, set $P_{\mathrm{e}}^{*}=0$. If the vehicle speed tends to exceed the maximum speed $v_{\max}$, brake operation will be taken. Note that the EMP and KEC controllers established the analytical control laws (19) and (24), containing simple algebraic and logic operations only. This feature leads to a very light computing load, which even can be neglected.

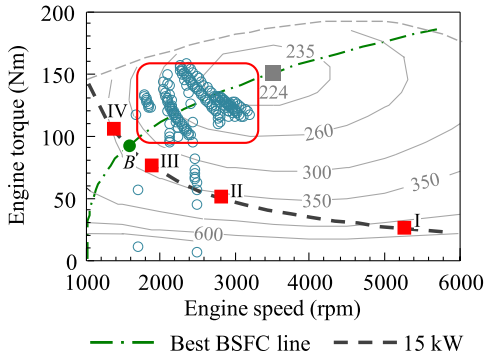

Fig. 5. Engine operating points of EMP controller for the AMT-type vehicles.

D. Control Law of Gear Selection

Based on the designed control rules of engine power P_{e} and brake force B under the continuous-gear assumption, this section aims at designing the gear selection law of AMT.

Due to the discrete gear ratio of AMT, we cannot operate the engine on the best BSFC line as a vehicle with an ideal CVT. As shown in Fig. 5, if the demanded power is 15 kW and the vehicle speed is 12 m/s, the CVT-type vehicle can operate on point B with the best engine efficiency, while the AMT-type vehicle can only operate on one of the four points I to IV, corresponding to gear position I to IV.

In this paper, the gear is selected to maximize the engine efficiency η_{e} at the determined engine power P_{e}^{*} (e.g., gear III when $P_{\mathrm{e}}^{*}=15$ kW and $v=12$ m/s in Fig. 5), denoted as

$$i_{\mathrm{g}}^{*}=\arg\max_{i_{\mathrm{g}}}\left\{\eta_{\mathrm{e}}(w_{\mathrm{e}},T_{\mathrm{e}})|w_{\mathrm{e}}=k_w v i_{\mathrm{g}},T_{\mathrm{e}}=\frac{P_{\mathrm{e}}^{*}}{w_{\mathrm{e}}}\right\}. \tag{25}$$

Although this strategy is less rigorous, it is more implementable than solving nonlinear mixed-integer problem directly. Its main idea is to use the discrete gear ratio to approach/approximate a continuous gear ratio profile. An example and its performance are given in the next section.

E. Benchmarks

To show the fuel economy and computing load of the EMP and KEC controllers, the model predictive control (MPC) and the constant speed (CS) controller are selected as benchmarks with a brief introduction.

1) Model Predictive Control (MPC): The MPC is designed following the framework of [5] and [6]. At each step, to avoid the vehicle speed deviates from the desired speed v_{d}, a penalty term $\beta(v-v_{\mathrm{d}})^2$ is added into cost function, where β is the penalty coefficient. Then the eco-cruising problem (8) is converted to

$$\min\ J=\int_{s_i}^{s_i+s_{\mathrm{T}}}\frac{\mathcal{F}_{\mathrm{e}}(P_{\mathrm{e}})+\beta(v-v_{\mathrm{d}})^2}{v}\mathrm{d}s,$$

subject to

$$\begin{aligned}&\frac{\mathrm{d}v}{\mathrm{d}s}=\frac{1}{v}g(P_{\mathrm{e}},v,B,s),\\&s_i=i\cdot\Delta s,\qquad i=0,1,2,\ldots.\end{aligned} \tag{26}$$

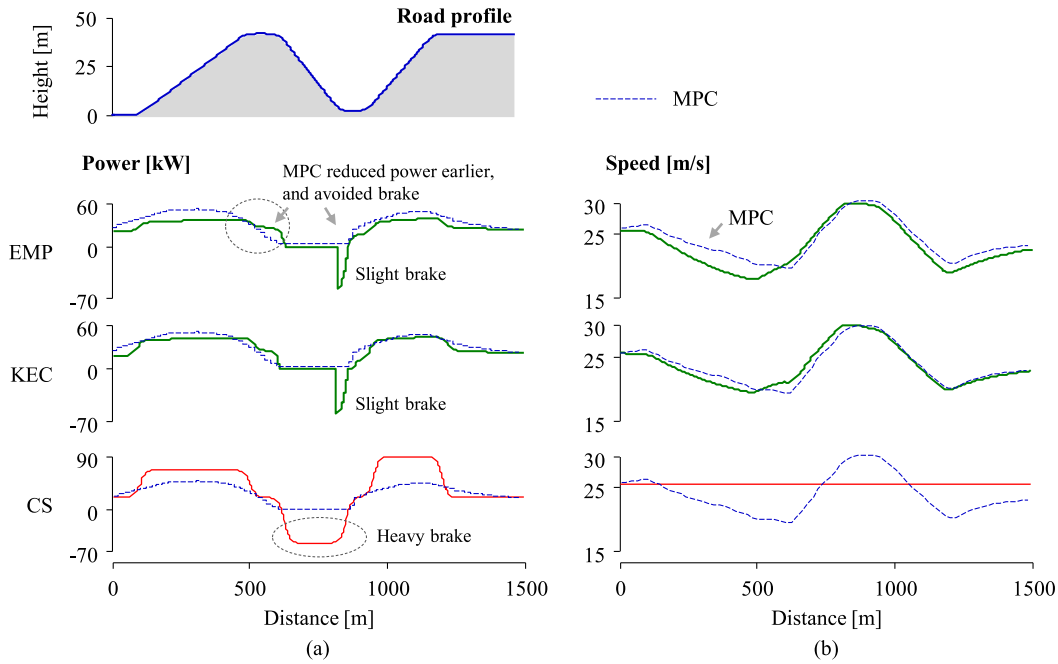

Fig. 6. Engine power and vehicle speed of the four controllers. (a) Engine power (in kilowatts). (b) Vehicle speed profile (in meters per second).

where s_{T} is the horizon, Δs is the step length, and s_i is the initial position of the ith step. The actual adopted control input in $[s_i, s_{i+1}]$ is the optimized engine power at point s_i. Here the parameters are set to $\Delta s = 5$ meters, $s_{\mathrm{T}} = 300$ meters referring to the existing studies. The penalty coefficient is set to $\beta = 0.01$, its effect on fuel economy is discussed in Section IV.

The algorithms of solving MPC are discussed in lots of existing works [8], [15]. However, the nonlinear constrained MPC is still challenging to solve in real time for fast dynamic systems [15]. In this paper, we ignore the issue of real-time computing, and use the Legendre-Gauss-Lobatto (LGL) pseudospectral method to solve it offline [24].

2) Constant Speed (CS) Controller: Constant speed (CS) controller that aims to maintain a fixed desired speed v_{d}, is also designed as a benchmark. It has a clear control law and is suitable for comparison. Denote the demanded power P_{d} of cruising on slope θ at v_{d} as

$$P_{\mathrm{d}}(v_{\mathrm{d}}) = \frac{v_{\mathrm{d}}}{\eta_{\mathrm{T}}} \left[r(v_{\mathrm{d}}) + h(s) \right] \tag{27}$$

where P_{d} can be positive or negative. It may exceed the physical limits of engine $(P_{\mathrm{e,max}})$ or brake system (P_{min}) on steep uphills or steep downhills, thus the actual adopted power P is set to

$$P = \begin{cases} P_{\mathrm{d}}, & v = v_{\mathrm{d}}, P_{\mathrm{d}} \in [P_{\mathrm{min}}, P_{\mathrm{e,max}}] \\ P_{\mathrm{e,max}}, & v < v_{\mathrm{d}} \text{ or } P_{\mathrm{d}} > P_{\mathrm{e,max}} \\ P_{\mathrm{min}}, & v > v_{\mathrm{d}} \text{ or } P_{\mathrm{d}} < P_{\mathrm{min}} \end{cases} \tag{28}$$

Note that the positive engine power P_{e} and negative brake force B are unified as one lumped control input P. If $P_{\mathrm{d}} \in [P_{\mathrm{min}}, P_{\mathrm{e,max}}]$, the vehicle will keep cruising at the fixed speed v_{d}. Otherwise, the vehicle speed v will deviate from v_{d}, and then the maximum engine power or minimum brake force will be adopted until v recovers to v_{d}. This control law is explicit and different from the widely-used PID control, whose performance depends on its coefficient setting.

IV. Performance of Controllers

First, a virtual road is adopted to show the effectiveness of the controllers. Then, a real highway from Chengdu to Chongqing in China is then employed to test the controllers. To show the of the KEC and EMP, two indexes, i.e., fuel saving rate and computing load, are quantitatively compared, along with a qualitative explanation for the results.

A. Cruising on a Virtual Road

The virtual road consists of two up-hills and one down-hill, as shown in Fig. 6. The initial speed v_0 is set to the economical speed of cruising on a flat road, i.e., 25.6 m/s. The vehicle speed is limited to the range of [15, 30] m/s. The resulting engine power and vehicle speed profiles of the four controllers are shown in Fig. 6, where the brake force is converted into negative engine power.

The resulting engine torque and gear sequence of AMT are shown in Fig. 7, as well as the optimal gear ratio and torque of the ideal CVT-type vehicle. We can observe that the discrete gear ratio and the corresponding engine torque are approaching the continuous ones in the form of "piecewise approximation". The resulting engine operating points are shown in Fig. 5, which indicates that the engine of AMT-type vehicle operates near the best BSFC line and in the high efficiency region.

In Fig. 6, on the first up-hill, the vehicle speeds of the MPC, EMP, and KEC drop first, even though the engine powers are high. On the down-hill, the vehicle speeds increase quickly, the engine powers fall to zero and brake operations are even adopted to avoid hypervelocity (i.e., 30 m/s). On the second up-hill, the vehicle speeds drop again and the engine power restores.

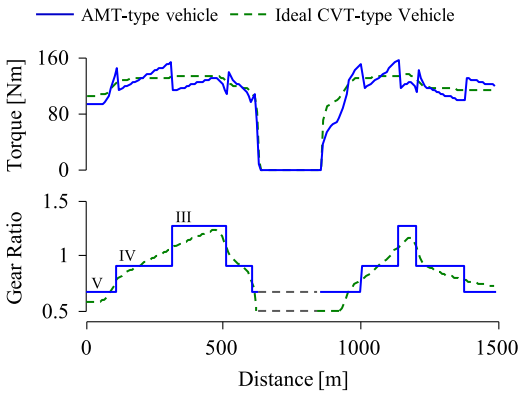

Fig. 7. Gear sequence and engine torque profile of the EMP controller.

TABLE II
RESULTS OF CRUISING ON THE VIRTUAL ROAD

Controller	MPC	EMP	KEC	CS
Initial v (m/s)	25.6	25.6	25.6	25.6
Final v (m/s)	22.84	22.65	22.82	25.6
Travel time (s)	64.6	67.2	65.22	58.9
Total fuel $J_{\#}$ (g)	126.9	128.7	129.6	177.6

The MPC controller with prediction capacity can reduce engine power earlier at the end of the first up-hill, which avoids the kinetic-energy-consuming brake operation on the following down-hill. However, the EMP and KEC controllers suffer a mild energy waste from the brake operations. The CS controller that tries to maintain a constant speed, employs a heavy brake on the downhill and inefficient high engine power on the up-hills, leading to the worst fuel economy.

As shown in Table II, the EMP and KEC controllers consume similar fuel to the MPC, and much less fuel than the CS. However, the fuel consumption values are less comparable due to the short mileage and different final speeds; a more convincing comparison is given in Section IV-B.

Remark 1: In the MPC, the fuel economy is affected by β, the coefficient to penalize speed deviation. To have a fair comparison, β has been set to a near-optimal value. The fuel consumption under different β is shown in Fig. 8. The final speeds v_{f} are limited to a same value (i.e., 22.84 m/s). The speed deviation V_{g} as compared with the desired speed v_{d} is also given in Fig. 8, defined as

$$V_{\mathrm{g}} = \frac{1}{s_{\mathrm{f}} - s_0} \int_{s_0}^{s_{\mathrm{f}}} |v - v_{\mathrm{d}}| \mathrm{d}s. \tag{29}$$

Fig. 8 shows that the higher β, the lower speed deviation, and the higher fuel consumption. The setting $\beta = 0.01$ is a near-optimal value for the MPC to achieve high fuel economy.

Remark 2: The range of vehicle speed (i.e., $v \in [15, 30]$ m/s) also affects the fuel economy, but it does not change the order of fuel saving. If we change the range to [10, 20], [20, 30], and [30, 40] m/s, the performances of the four controllers are shown in Fig. 9. It indicates that (a) the order of fuel economy does not change in different ranges, i.e., MPC $>$ EMP $\approx$ KEC $>$ CS; (b) if the speed range becomes narrower, the fuel economy becomes worse; improper speed level also deteriorates fuel economy.

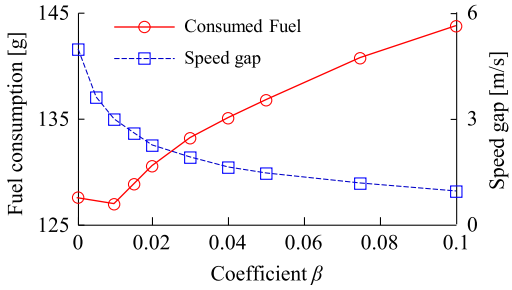

Fig. 8. Fuel economy of the MPC under different penalty coefficient β.

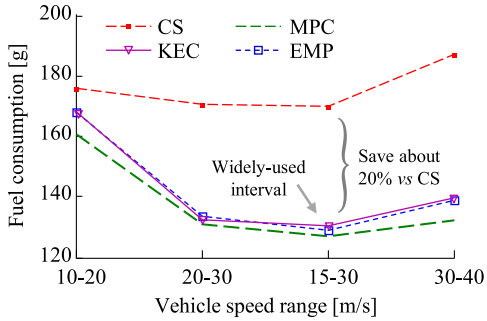

Fig. 9. Effect of speed range on fuel-saving performance.

TABLE III
SIMULATION RESULTS OF CRUISING ON THE HIGHWAY G76

Controller	MPC	EMP	KEC	CS
Travel time /min	128	120	128	118
Average Computing Time per step /ms	--	0.40	0.22	0.21
Fuel (ideal-CVT) /kg	11.02	11.52	11.15	12.83
Fuel (AMT) /kg	11.24	11.79	11.34	13.22
Fuel Saving Rate η_F	-15.0%	-10.8%	-14.2%	B.M.

B.M.: Benchmark

B. Cruising on a Real Highway

To persuasively compare the controllers, the highway G76 between Chengdu and Chongqing is selected and simulated. Its mileage is 180 km; the road profile is shown in Fig. 10(a). The mentioned four controllers, MPC, EMP, KEC, and CS, are used respectively. The speed range is set to $v \in [15, 30]$ m/s, and v_0 and v_{d} is set to the economical speed 25.6 m/s.

The resulting vehicle speed is shown in Fig. 10(b), and the profiles of 11-14 km are enlarged as Fig. 10(c). The speed of CS is close to the desired speed v_{d} except for the steep uphill section. The speed of MPC is smoother with smaller fluctuation as compared with the EMP and the KEC. The demanded traveling time of the four controllers are around 2 hours with a maximal gap of 10 minutes.

Especially, the two main performance indexes, i.e., fuel saving rate and computing load, are shown in Table III. The fuel saving rate is defined as

$$\eta_F = \frac{J_{\#} - J_{\mathrm{CS}}}{J_{\mathrm{CS}}} \times 100\% \tag{30}$$

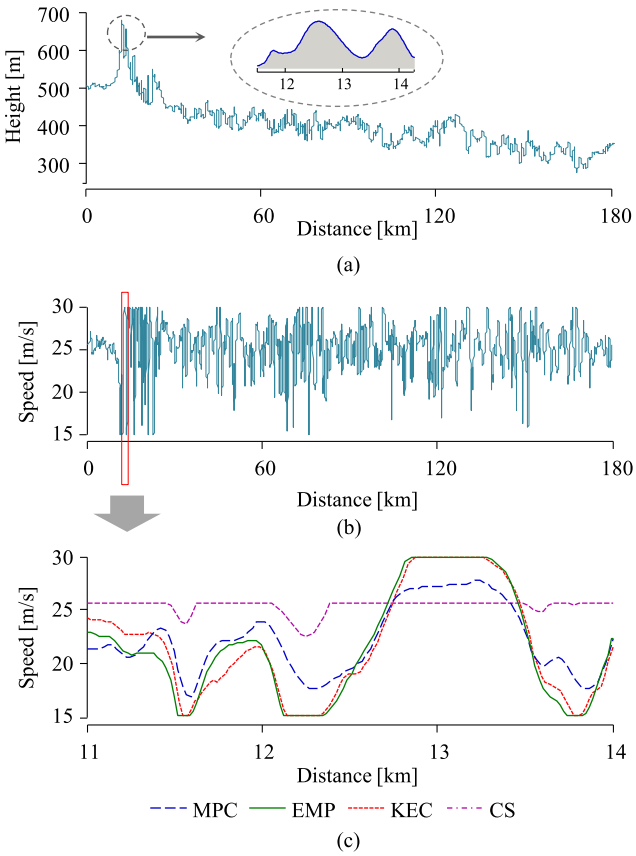

Fig. 10. Control results of cruising on the highway between Chengdu and Chongqing. (a) Road profile. (b) Vehicle speed profiles. (c) Speed profiles of 11–14 km.

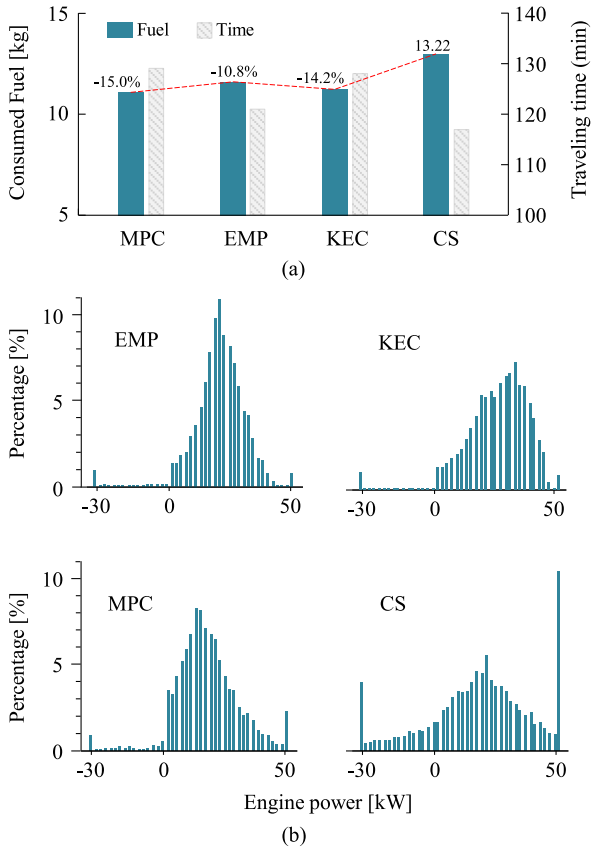

Fig. 11. Comparison of the four controllers on the highway. (a) Fuel consumption and traveling time. (b) Distribution of engine power/brake power.

where $J_{\#}$ stands for the total fuel consumption of the MPC, EMP, and KEC. The computing load is evaluated by the average computing time per step. The total fuel consumption of the AMT-type vehicle and the ideal-CVT-type vehicle is also shown in Table III. Based on the results, three points are discussed below:

(1) The fuel saving rates of EMP and KEC are a little lower but close to that of MPC. Fig. 11(a) shows that the EMP and KEC achieve 10.8% and 14.2% fuel saving as compared with the CS, respectively; while the MPC saves 15.0% fuel. Therefore, the designed controllers have similar fuel economy to the MPC, and achieve more than 10% fuel savings than the CS.

The results can be explained by the power distribution, as shown in Fig. 11(b). The CS controller uses more brake operations and more "high engine power", while the most engine power of other controllers fall into the economical range of [15, 35] kW, and brake operation is rarely used.

(2) The EMP and KEC controllers have very light computing load. Their average computing time of each step is less than 0.5 milliseconds, which is in the same level of the rule-based CS controller. While the MPC controller needs more time to solve the nonlinear optimization problem, which depends on the employed algorithm. In this paper, the LGL pseudo-spectral method is adopted and the computing time is in the level of about 5 seconds. Note that it is not a very fast method for solving MPC problem, thus its computing time cannot be used for fair comparison. In general, the EMP and KEC with analytical laws have much lower computing load than the optimization-based MPC, making them become a new option for eco-cruising systems.

(3) The AMT-type vehicle and the ideal-CVT-type vehicle have the same trend and a minor difference on fuel consumption, as shown in Table III. The former consumes roughly more 3% fuel than the latter due to the discrete gear ratio. The small incremental indicates the effectiveness of the designed gear selection strategy in Section III-D.

C. Qualitative Explanation

To explain the difference of the controllers' fuel economy, a qualitative analysis is given below. Generally, the performance of fuel saving depends on the following two factors:

(a) Ability of "slope adaptation", that is the capability of selecting a proper cruising speed for a given slope. As shown in Fig. 4, a specific slope corresponds to a specific fuel-optimal cruising speed. If the vehicle speed deviates from the optimum, the fuel economy will deteriorate. The controllers should make the vehicle speed approach to the fuel-optimal speed.

(b) Ability of "prediction", that is to program vehicle speed with the future information, which can avoid inefficient operations. For example, on the steep downhill in

Fig. 6, the MPC can decrease the engine power earlier before the downhill, and thus avoid unnecessary brake; while the other three controllers do not have this ability.

Generally, the EMP and KEC have better slope adaptation than the MPC under the given framework, but they also fully lose the ability of prediction. Since the EMP/KEC and the MPC have their own merits respectively, their fuel-saving performances are close to each other. The CS controller loses the both abilities, thus ending up the worst fuel economy.

Note that: (a) the MPC controller's slope adaptation ability is related to β; generally, the smaller β the better slope adaptation, and thus the better fuel economy, as shown in Fig. 8. (b) The vehicle speed range, i.e., $v_{\min} \le v \le v_{\max}$, affects the slope adaptation ability of all controllers; too tight range will dent optimization space and thus weaken the fuel economy, as shown in Fig. 9. We emphasize that both the EMP/KEC and the MPC have their own advantages in computing load or fuel economy; designers could choose a proper one according to their preferences.

V. Controller Expansion to Car-Following Scenarios

Driving safety is always the paramount requirement, and any eco-driving operation should make a concession to it. If a vehicle is cruising with a slow frontal vehicle, its economical operation may be impeded. Thus the front vehicle that might cause rear-end collision, actually becomes a constraint. This section discusses how to expand the designed controllers EMP and KEC to the impeded scenarios.

If there is no leading vehicle, the hosting vehicle can cruise using the economical acceleration a_{eco} obtained by the EMP or KEC controller. When the vehicle is impeded, the applied acceleration should be lower than the safety-guaranteed acceleration a_s. Here we adopt the Gipps car-following model to estimate the maximum safe acceleration a_s [25]. The Gipps model shows that if the hosting/frontal vehicle has a maximum deceleration b_h/b_f, the maximum safe acceleration a_s enabling collision avoidance is estimated from

$$\begin{aligned} a_s(t) &= \frac{v_h(t+\tau) - v_h(t)}{\tau}, \\ v_h(t+\tau) &= b_h\tau + \left[b_h^2\tau^2 - 2b_h(x_f - x_h - D_s)\right. \\ &\quad \left. + b_h v_h(t)\tau + b_h v_f^2/b_f\right]^{0.5} \end{aligned} \tag{31}$$

where v_h and x_h (v_f and x_f) are the speed and location of the hosting (frontal) vehicle; τ is the reaction time; D_s is the safe distance of two adjacent vehicles when they are stationary, including the length of vehicle body.

Combining the safety-guaranteed acceleration a_s and the fuel-prioritized acceleration a_{eco}, the applied acceleration is given by

$$a(t) = \min(a_{\text{eco}}, a_{\text{s}}). \tag{32}$$

In the following case study, the parameters are set as $\tau = 0.55$ s, $D_s = 9$ m, and $b_{\#} = -2$ m/s^2 without considering the effect of road slope (i.e., roughly in the range of $[-0.3, 0.3]$ m/s^2). The frontal vehicle is assumed to cruise at 20 m/s when $x_l < 750$ m, and then turn to 13 m/s, as shown in Fig. 12. The initial

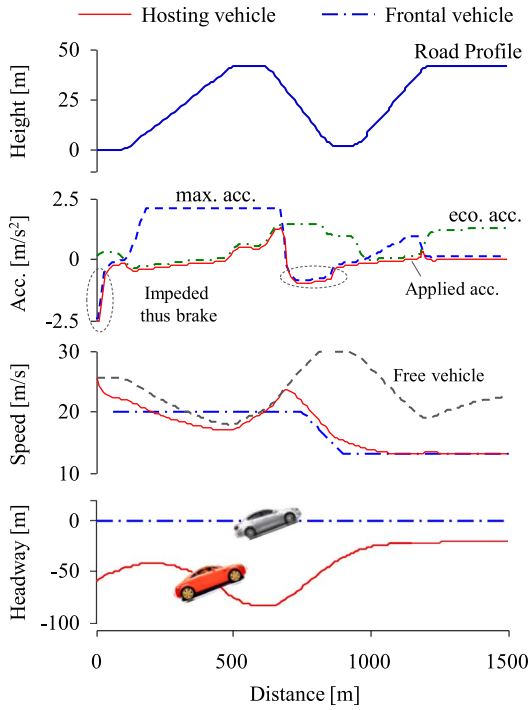

Fig. 12. Computing results of eco-cruising with a slow frontal vehicle.

speed and headway of the hosting vehicle are set to 25.6 m/s and 60 m. By using the EMP controller and the above rule (32), the resulting profiles of acceleration, speed, and headway are shown in Fig. 12.

The headway profile shows that the hosting vehicle never collided with the frontal vehicle. At the beginning, the impact risk is high due to the short distance gap and high negative speed gap, thus an uneconomic brake operation is adopted to decrease the risk. At $x_l = 750$ m, the frontal vehicle suddenly decelerates to 13 m/s and the impact risk becomes higher again, which ends up another brake operation. The lower speed that deviates from the optimum, leads to lower engine efficiency and inevitably deteriorates the fuel economy. In this case, the impeded vehicle (150.2 g) consumed more 16.7% fuel than the free vehicle (128.7 g) without considering the difference in final speeds.

This strategy does not need on-line optimization and prediction of frontal vehicles' motion, which is practical for automated vehicles to implement eco-cruising in real traffic system, especially in the early intelligent transportation systems where automated vehicles and unpredictable human-driven vehicles coexist.

VI. Conclusion

This paper designed two feedback controllers for fuel-prioritized cruising system with known road slope information, i.e., estimated minimum principle (EMP) and kinetic-energy conversion (KEC). Different from the optimization-based control with look-ahead information, the designed controllers have analytical control laws and rely on current road slope only, which leads to very light computing load. The average computing time of each step is less than 0.5 milliseconds, in the same

level of the rule-based CS control. This feature meets the requirement of online implementation in real traffic system. Their fuel-economies are about 1–4% lower than the optimization-based MPC controller when tested on a 180 km highway, and 10–15% better than the CS controller that aims at maintaining a fixed vehicle speed. The light computing load and high fuel economy make them a new option for online eco-cruising control systems.

Generally, the designed controllers could be integrated into automated vehicles or adaptive cruise control (ACC) systems to further decrease fuel consumption. It is worth noting that other factors such as traffic signal also affect the implementation of eco-cruising, which are not considered in this paper.

REFERENCES

[1] E. W. Martin and S. A. Shaheen, "Greenhouse gas emission impacts of carsharing in North America," *IEEE Trans. Intell. Transp. Syst.*, vol. 12, no. 4, pp. 1074–1086, Mar. 2011.

[2] A. E. Atabani, I. A. Badruddin, S. Mekhilef, and A. S. Silitonga, "A review on global fuel economy standards, labels and technologies in the transportation sector," *Renewable Sustain. Energy Rev.*, vol. 15, no. 9, pp. 4586–4610, 2011.

[3] S. E. Li, S. Xu, X. Huang, B. Cheng, and H. Peng, "Eco-departure of connected vehicles with V2X communication at signalized intersections," *IEEE Trans. Veh. Technol.*, vol. 64, no. 12, pp. 5439–5449, Dec. 2015.

[4] H. Y. Tong, W. T. Hung, and C. S. Cheung, "On-road motor vehicle emissions and fuel consumption in urban driving conditions," *J. Air Waste Manage. Assoc.*, vol. 50, no. 4, pp. 543–554, 2000.

[5] E. Hellström, M. Ivarsson, J. Åslund, and L. Nielsen, "Look-ahead control for heavy trucks to minimize trip time and fuel consumption," *Control Eng. Pract.*, vol. 17, no. 2, pp. 245–254, 2009.

[6] M. A. S. Kamal, M. Mukai, J. Murata, and T. Kawabe, "Ecological vehicle control on roads with up-down slopes," *IEEE Trans. Intell. Transp. Syst.*, vol. 12, no. 3, pp. 783–794, Sep. 2011.

[7] C. Lin, H. Peng, J. W. Grizzle, and J. Kang, "Power management strategy for a parallel hybrid electric truck," *IEEE Trans. Control Syst. Technol.*, vol. 11, no. 6, pp. 839–849, Nov. 2003.

[8] T. Ohtsuka, "A continuation/GMRES method for fast computation of nonlinear receding horizon control," *Automatica*, vol. 40, no. 4, pp. 563–574, 2004.

[9] S. Di Cairano, D. Bernardini, A. Bemporad, and I. V. Kolmanovsky, "A stochastic MPC with learning framework for driver-aware vehicle control, and its application to HEV energy management," *IEEE Trans. Control Syst. Technol.*, vol. 22, no. 3, pp. 1018–1031, May 2014.

[10] H. Borhan, A. Vahidi, A. Phillips, M. Kuang, I. V. Kolmanovsky, and S. Di Cairano, "MPC-based energy management of a power-split hybrid electric vehicle," *IEEE Trans. Control Syst. Technol.*, vol. 20, no. 3, pp. 593–603, May 2012.

[11] L. Johannesson, S. Pettersson, and B. Egardt, "Predictive energy management of a 4QT series-parallel hybrid electric bus," *Control Eng. Pract.*, vol. 17, pp. 1440–1453, 2009.

[12] A. Sciarretta and L. Guzzella, "Control of hybrid electric vehicles," *IEEE Control Syst. Mag.*, vol. 27, no. 2, pp. 60–70, Apr. 2007.

[13] D. Shen, V. Bensch, and S. Miiller, "Model predictive energy management for a range extender hybrid vehicle using map information," *IFAC-PapersOnLine*, vol. 48, no. 15, pp. 263–270, 2015.

[14] M. Wahba and S. Brennan, "MPC-based energy management of a parallel hybrid electric vehicle using terrain information," presented at the ASME Dynamic Systems Control Conference, American Society Mechanical Engineers, Columbus, OH, USA, Oct. 2015.

[15] Y. Wang and S. Boyd, "Fast model predictive control using online optimization," *IEEE Trans. Control Syst. Technol.*, vol. 18, no. 2, pp. 267–278, Mar. 2010.

[16] P. Pisu and G. Rizzoni, "A comparative study of supervisory control strategies for hybrid electric vehicles," *IEEE Trans. Control Syst. Technol.*, vol. 15, no. 3, pp. 506–518, May 2007.

[17] C. Musardo, G. Rizzoni, and B. Staccia, "A-ECMS: An adaptive algorithm for hybrid electric vehicle energy management," in *Proc. IEEE Conf. Decision Control*, 2005, pp. 1816–1823.

[18] A. B. Schwarzkopf and R. B. Leipnik, "Control of highway vehicles for minimum fuel consumption over varying terrain," *Transp. Res.*, vol. 11, no. 4, pp. 279–286, 1977.

[19] A. Froberg and L. Nielsen, "Optimal fuel and gear ratio control for heavy trucks with piece wise affine engine characteristics," *Adv. Automotive Control*, vol. 5, no. 1, pp. 335–342, 2007.

[20] S. Xu, S. E. Li, X. Zhang, B. Cheng, and H. Peng, "Fuel-optimal cruising strategy for road vehicles with step-gear mechanical transmission," *IEEE Trans. Intell. Transp. Syst.*, vol. 16, no. 6, pp. 3496–3507, Dec. 2015.

[21] L. Guzzella and A. Sciarretta, *Vehicle Propulsion Systems: Introduction to Modeling and Optimization*. New York, NY, USA: Springer, 2005, pp. 15–16.

[22] S. E. Li and H. Peng, "Strategies to minimize the fuel consumption of passenger cars during car-following scenarios," *Proc. Inst. Mech. Eng. D, J. Automobile Eng.*, vol. 226, no. 3, pp. 419–429, 2012.

[23] G. Genta, *Motor Vehicle Dynamics-Modelling and Simulation*. London, U.K.: World Scientific, 1997, pp. 205–274.

[24] S. Xu, S. E. Li, K. Deng, S. Li, and B. Cheng, "A unified pseudospectral computational framework for optimal control of road vehicles," *IEEE/ASME Trans. Mechatronics*, vol. 20, no. 4, pp. 1499–1510, Aug. 2015.

[25] P. G. Gipps, "A behavioural car-following model for computer simulation," *Transp. Res. B, Methodol.*, vol. 15, no. 2, pp. 105–111, 1981.

Shaobing Xu received the B.S. degree in automotive engineering from China Agricultural University, Beijing, China, in 2011, and the Ph.D. degree in mechanical engineering from Tsinghua University, Beijing, in 2016.

In 2014, he was a Visiting Scholar with University of Michigan, Ann Arbor, MI, USA. He is currently with the State Key Laboratory of Automotive Safety and Energy, Department of Automotive Engineering, Tsinghua University. His research interests include optimal control theory, decision/control of automated vehicles, and vehicle dynamics control.

Mr. Xu was a recipient of the National Scholarship, the President Scholarship, the First Prize of the Chinese Fourth Mechanical Design Contest, and the First Prize of the 19th Advanced Mathematical Contest.

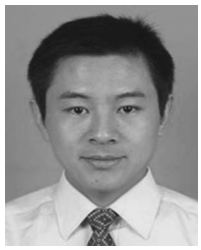

Shengbo Eben Li (M'11) received the M.S. and Ph.D. degrees from Tsinghua University, Beijing, China, in 2006 and 2009, respectively.

In 2007, he was a Visiting Scholar with Stanford University, Stanford, CA, USA. From 2010 to 2011, he was a Postdoctoral Research Fellow with University of Michigan, Ann Arbor, MI, USA. In 2015, he was a Visiting Research Scientist with University of California, Berkeley, Berkeley, CA, USA. He is currently an Associate Professor with the Department of Automotive Engineering, Tsinghua University. His active research interests include automated connected vehicles, optimal control and multiagent control, driver behavior and driver assistance, and lithium-ion battery management.

Prof. Li was the recipient of the Award for Science and Technology of China ITS Association (2012), the Award for Technological Invention in the Ministry of Education (2012), the National Award for Technological Invention in China (2013), and the Honored Funding for Beijing Excellent Youth Researcher (2013).

Bo Cheng received the B.S. and M.S. degrees in automotive engineering from Tsinghua University, Beijing, China, in 1985 and 1988, respectively, and the Ph.D. degree in mechanical engineering from Tokyo University, Tokyo, Japan, in 1998.

He is now a Professor and the Dean with the Suzhou Automotive Research Institute, Tsinghua University. His active research interests include autonomous vehicles, driver-assistance systems, active safety, and vehicular ergonomics.

Prof. Cheng is the Chairman of the Academic Board of SAE-Beijing, a Member of the Council of Chinese Ergonomics Society, and a Committee Member of the National 863 Plan.

Keqiang Li received the B.Tech. degree from Tsinghua University, Beijing, China, in 1985, and the M.S. and Ph.D. degrees from Chongqing University, Chongqing, China, in 1988 and 1995, respectively.

He is a Professor in automotive engineering with Tsinghua University. He has authored over 90 papers and is a coinventor on 12 patents in China and Japan. His research interests include vehicle dynamics, control for driver-assistance systems, and hybrid electrical vehicles.

Dr. Li is a Senior Member of the Society of Automotive Engineers of China and is on the editorial boards of *International Journal of Intelligent Transportation Systems Research* and *International Journal of Vehicle Autonomous Systems*. He has the recipient of the Changjiang Scholar Program Professor Award and of some awards from public agencies and academic institutions of China.